Translational correlations in the vortex array at the surface of a type-II superconductor

M. Cristina Marchetti
Physics Department, Syracuse University, Syracuse, New York 13244

David R. Nelson
Lyman Laboratory of Physics, Harvard University, Cambridge, Massachusetts 01238
(Received 10 December 1992)

We discuss the statistical mechanics of magnetic flux lines in a finite-thickness slab of type-II superconductor. The long-wavelength properties of a flux-line liquid in a slab geometry are described by a hydrodynamic free energy that incorporates the boundary conditions on the flux lines at the sample's surface as a surface contribution to the free energy. Bulk and surface weak disorder are modeled via Gaussian impurity potentials. This free energy is used to evaluate the two-dimensional structure factor of the flux-line tips at the sample surface. We find that surface interaction always dominates in determining the decay of translational correlations in the asymptotic long-wavelength limit. On the other hand, such large length scales have not been probed by the decoration experiments. Our results indicate that the translational correlations extracted from the analysis of the Bitter patterns are indeed representative of behavior of flux lines in the bulk.

I. INTRODUCTION

The nature of the ordering of the magnetic-flux array in the mixed state of high-temperature copper oxide superconductors has received considerable experimental and theoretical attention in the last few years. It has been shown that fluctuations are important in these materials and can lead to a number of new phases or regimes of the flux array, including entangled flux liquids, hexatic flux liquids,[1,2] and hexatic vortex glasses.[3,4] Most experiments probe the properties of the flux array indirectly by measuring bulk properties of the superconductors, such as transport, magnetization, or mechanical dissipation. At present direct measurements of the microscopic order of the magnetic-flux array are mainly limited to decoration experiments at low fields.[5–9] These experiments aim to extract information on the vortex line configurations in the bulk of the material by imaging the pattern of the magnetic-flux lines as they emerge at the surface of the sample. The surface patterns are determined by the interplay of thermal fluctuations and impurity disorder. Both these mechanisms can be responsible for disrupting translational and orientational order of vortex arrays.[10,11] Surface roughness can also play a role in determining the surface magnetic patterns. It is clear that to interpret the experiments and assess whether one can indeed consider the surface patterns as representative of vortex line configurations in the bulk of the sample, one needs to understand what are the relative effects of bulk-versus-surface interactions and disorder in determining the configuration of the vortex tips as they emerge at the surface. Almost 30 years ago, Pearl[12] showed that the interaction between the tips of straight flux lines at a superconductor-vacuum interface decays as $1/r_\perp$ at large distances, with $r_\perp$ the distance between flux tips along the interface. In contrast, the interaction between flux-line elements in bulk decays exponentially at large distances. For this reason Huse has questioned the assumption that surface patterns are representative of flux-line configurations in the bulk and has argued that at low fields, where the intervortex separation is large compared to the penetration length, surface effects may play the dominant role in determining the magnetic-flux patterns seen at the surface.[13]

By analyzing flux decoration images one can extract quantitative information on the decay of both translational and orientational correlations of flux-line tips at the sample surface. In this paper we focus on the long-wavelength behavior of translational correlations in the flux-line liquid phase. This case may be relevant to the interpretation of decoration experiments such as those by the AT&T group[9] for the following reason. The decoration experiments are carried out by quenching the sample in a small field from high to low temperature. The observed flux patterns do not represent the equilibrium configurations of vortices at the low temperature where the decoration takes place, but equilibrium configurations corresponding to a higher temperature, T_f, where the flux array falls out of equilibrium. While the value of T_f is not known, there are indications that it may be near the irreversibility line, $T_{\rm irr}$, which in turn has been found to be very close to T_c at low fields in the Bi-Sr-Ca-Cu-O samples used for the decorations.[9] The experiments may then be probing a rather narrow range of temperatures between $T_{\rm irr}$ and T_f where the flux array is in the polymerlike state proposed by Nelson and Seung.[14] The long-wavelength static properties of such a glassy polymer can be described in terms of a hydrodynamic flux-line liquid free energy.[1]

Translational correlations of flux lines in three dimensions are described by the density-density correlation function. For convenience we consider the Fourier transform of this correlation function in the plane normal to the applied field,

$$n_0 S(q_\perp,z_1,z_2)=\overline{\langle \delta n(\mathbf{q}_\perp,z_1)\delta n(-\mathbf{q}_\perp,z_2)\rangle} - \overline{\langle \delta n(\mathbf{q}_\perp,z_1)\rangle\langle \delta n(-\mathbf{q}_\perp,z_2)\rangle}\ , \quad (1.1)$$

where $n(\mathbf{q}_\perp,z)$ is the in-plane Fourier transform of the coarse-grained flux-line density,

$$n(\mathbf{r}_\perp,z)=\sum_{i=1}^{N}\delta(\mathbf{r}_\perp-\mathbf{r}_i(z))\ . \quad (1.2)$$

Here $\mathbf{r}_i(z)$ is the position of the ith vortex in the (x,y) plane as it wanders along the $\hat{\mathbf{z}}$ ($\hat{\mathbf{z}}\|\mathbf{H}$) axis and $\delta n(\mathbf{r}_\perp,z)=n(\mathbf{r}_\perp,z)-n_0$ denotes the fluctuation of the local density from its equilibrium value, $n_0=B/\phi_0$, with B the average induction at equilibrium and ϕ_0 the flux quantum. The angular brackets denote a thermal average and the overbar the average over quenched impurity disorder. The subtracted term on the right-hand side of Eq. (1.1) vanishes in the absence of quenched disorder.

The two-dimensional structure function of a constant-z cross section of flux liquid is obtained from (1.1) by letting $z_1=z_2$,

$$n_0 S_2(q_\perp,z_1)=\overline{\langle|\delta n(\mathbf{q}_\perp,z_1)|^2\rangle}-|\overline{\langle\delta n(\mathbf{q}_\perp,z_1)\rangle}|^2\ . \quad (1.3)$$

A factor of n_0 has been extracted from the definition of the structure function so that $S_2(q_\perp,z_1)\to 1$ as $q_\perp\to\infty$, for all values of z_1.

The behavior of the flux-line structure function (1.1) for bulk flux-line liquids in the presence of both thermal fluctuations and quenched disorder has been discussed before.[15] In an infinitely thick superconductor the correlation of density fluctuations at different heights only depends on the distance, $|z_1-z_2|$. The results are then most conveniently discussed in terms of the full three-dimensional structure function obtained by Fourier transforming (1.1) with respect to z_1-z_2,

$$n_0 S(q_\perp,q_z)=\overline{\langle|\delta n(\mathbf{q}_\perp,q_z)|^2\rangle}-|\overline{\langle\delta n(\mathbf{q}_\perp,q_z)\rangle}|^2\ . \quad (1.4)$$

For simplicity we only discuss in this section the contribution to the structure factor from thermal fluctuations, $S_T(q_\perp,q_z)$. This is easily calculated in the long-wavelength limit from a simple hydrodynamic theory,[1,15] with the result,

$$S_T(q_\perp,q_z)=\frac{n_0 k_B T q_\perp^2}{q_\perp^2 c_L(q_\perp,q_z)+q_z^2 c_{44}(q_\perp,q_z)}\ , \quad (1.5)$$

where $c_L(q_\perp,q_z)$ and $c_{44}(q_\perp,q_z)$ are the wave-vector-dependent compressional and tilt moduli of a bulk flux-line liquid, as given, for instance, in Ref. 1. In the long-wavelength limit one can invert the q_z transform by approximating the elastic constants in (1.5) with their values at $q_z=0$, with the result,

$$S_T(q_\perp,z_1-z_2)=\frac{n_0 k_B T}{B_3(q_\perp)\xi_\|(q_\perp)}e^{-|z_1-z_2|/\xi_\|(q_\perp)}\ , \quad (1.6)$$

where

$$\xi_\|(q_\perp)=\sqrt{K(q_\perp)/B_3(q_\perp)}\frac{1}{q_\perp} \quad (1.7)$$

is the correlation length describing the decay of correlations in the z direction, with $B_3(q_\perp)=c_L(q_\perp,0)$ and $K(q_\perp)=c_{44}(q_\perp,0)$. The asymptotic long-wavelength ($q_\perp\to 0$) behavior of the correlation function is determined by the constant values of the moduli at zero wave vector, $B_3(0)=B^2/4\pi$ and $K(0)=B^2/4\pi+\tilde{c}_{44}(0)$, where $\tilde{c}_{44}(0)$ is the tilt coefficient of a single line at $q_z=0$.[16] On the other hand, the nonlocality of the elastic constants is often important in the high-T_c superconductors even at small wave vectors because of the large values of the penetration lengths.[17]

Correlations in any constant-z cross section of the bulk are described by the two-dimensional structure factor defined in Eq. (1.3) and do not depend on z_1. The contribution to this two-dimensional structure factor from thermal fluctuations is immediately obtained by letting $z_1=z_2$ in Eq. (1.6),

$$S_{2T}(q_\perp)=\frac{n_0 k_B T}{B_3\xi_\|(q_\perp)}=\frac{n_0 k_B T}{\sqrt{KB_3}}q_\perp\ . \quad (1.8)$$

According to a well-known sum rule that relates the value of the structure factor at zero wave vector to the bulk modulus of the liquid, the denominator on the right-hand side of the first equality of Eq. (1.8) can be interpreted as an effective two-dimensional bulk modulus. This effective bulk modulus diverges in the long-wavelength limit, due to the divergence of the correlation length $\xi_\|$. As a consequence the two-dimensional structure factor of any constant-z cross section of a bulk flux-line liquid vanishes linearly as $q_\perp\to 0$. As discussed elsewhere,[15,18] this behavior arises here from the constraint that flux lines cannot start nor terminate inside the sample.

Decoration experiments measure correlations of flux lines in a constant-z cross section at the surface of a sample of finite thickness L. Most researchers have implicitly assumed that these surface correlations are representative of correlations in a constant-z cross section of bulk. If this is the case, Eq. (1.8) should describe the correlations of flux-line tips at the surface as extracted from the decoration experiments. On the other hand, it is clear that whenever $\xi_\|\gtrsim L$ finite-size effects may become important. Since $\xi_\|(q_\perp)$ diverges as $q_\perp\to 0$, finite-size effects may in fact dominate the long-wavelength behavior. In addition, we have mentioned that in a finite-size sample the boundary conditions modify the pair interaction between flux lines at the surface. The boundary conditions are determined by the requirement that on length scales larger than the penetration length the spatially uniform magnetic field outside the sample must equal the field of the vortex tips at the surface. In other words, the superconductor surface can be thought of as the boundary between a strongly anisotropic magnetic medium where the field is concentrated in the flux lines and an isotropic magnetic medium (the vacuum). At the surface the flux tips then behave like magnetic monopoles of "charge" $\phi_0/2\pi$ and therefore interact at large distances via a repulsive Coulomb-like potential, $V_s(r_\perp)=(\phi_0/2\pi)^2(1/r_\perp)$. The two-dimensional correlations of flux-line tips as they leave the sample could then be very different from those in a constant-z cross section

deep in the bulk. If in fact the long-range surface interaction would dominate in determining long-wavelength surface properties,[13] then decorations would image the configurations of a two-dimensional liquid of vortices interacting via a $1/r_\perp$ potential. The long-wavelength bulk modulus of such a two-dimensional liquid is $B_2(q_\perp)\simeq B^2/(4\pi q_\perp)$. The corresponding two-dimensional structure factor is given by $S_{2T}(q_\perp)=n_0k_BT/B_2(q_\perp)$ and again vanishes linearly as $q_\perp\to 0$, but with a different slope from the result of Eq. (1.8). A more detailed analysis is clearly needed to discriminate between these two possibilities.

In this paper we describe a model that can be used to study the long-wavelength properties of flux arrays in finite-size samples incorporating the appropriate boundary conditions for the flux lines at the sample surface. We consider a slab of a uniaxial anisotropic type-II superconductor. The field is applied along the $\hat{c}$ axis of the superconductor which is chosen as the z direction. The slab is infinite in the xy plane and has thickness L in the z direction. The starting point for the calculation presented here is a model hydrodynamic free energy that is a simplified version of the full hydrodynamic free energy obtained in Ref. 19. In essence we neglect any nonlocality and spatial inhomogeneity in the z direction other than the presence of the sample boundaries. The free energy is then written as the sum of a surface free energy, that incorporates the boundary conditions, and the usual hydrodynamic free energy of a bulk flux liquid. This free energy can be used as the starting point to study both how the coupling to the bulk affects the surface properties and how the bulk behavior is modified by the presence of the boundaries. In this paper we focus on translational correlations at the surface. Our main result is the two-dimensional structure factor at one of the surfaces of the sample. We find that the contribution to this structure factor from thermal fluctuations is given by,

$$S_{2T}(q_\perp,L)=\frac{n_0k_BT}{B_2^{\rm eff}(q_\perp,L)}\ , \tag{1.9}$$

where $B_2^{\rm eff}(q_\perp,L)$ is an effective two-dimensional surface bulk modulus,

$$B_2^{\rm eff}(q_\perp,L)=B_2(q_\perp)+B_3(q_\perp)\xi_\parallel(q_\perp)F(L/\xi_\parallel)\ , \tag{1.10}$$

with $B_2(q_\perp)\approx B^2/(4\pi q_\perp)$.[19] The crossover function F is given by

$$F(L/\xi_\parallel)=\frac{B_3\xi_\parallel+B_2\coth(L/\xi_\parallel)}{B_2+B_3\xi_\parallel\coth(L/\xi_\parallel)}\ . \tag{1.11}$$

If the ratio K/B_3 is large, as it can indeed be at the low fields used in the decoration experiments,[20] one can distinguish three regimes in the behavior of the effective surface bulk modulus as a function of the in-plane wave vector $q_\perp$,

$$\begin{aligned} B_2^{\rm eff}(q_\perp,L)&\sim B_2(q_\perp)\sim q_\perp^{-1},\quad q_\perp<\frac{1}{L}\\ &\sim LB_3\sim q_\perp^0,\quad \frac{1}{L}<q_\perp<q_\perp^*\\ &\sim\xi_\parallel B_3\sim q_\perp^{-1},\quad q_\perp>q_\perp^*\ . \end{aligned} \tag{1.12}$$

The crossover wave vector $q_\perp^*$ is defined as the wave vector where the correlation length $\xi_\parallel$ equals the sample size, $\xi_\parallel(q_\perp^*)=L$. For $q_\perp\to 0$ the correlation length $\xi_\parallel$ diverges and the flux lines are essentially rigid. The surface interaction dominates in this limit and the surface bulk modulus is simply that of a $2d$ liquid of magnetic monopoles. When $q_\perp>1/L$ and $\xi_\parallel>L$, corresponding to $q_\perp<q_\perp^*$, flux lines are still correlated in the z direction over the entire thickness of the sample, but the exponential interaction between straight flux lines in bulk dominates in this case and the surface modulus is LB_3. Finally, when $\xi_\parallel<L$, or $q_\perp>q_\perp^*$, flux lines are correlated over a length $\xi_\parallel$ smaller than the sample size and the surface bulk modulus is determined by the compressional energy per unit area of an array of essentially straight flux lines of length $\xi_\parallel$. The typical behavior of the surface structure factor as it crosses over from a linear function of $q_\perp$ at very small wave vectors to a linear function of $q_\perp$ with a smaller slope at large wave vectors is shown in Fig. 1. For both $q_\perp<1/L$ and $q_\perp>q_\perp^*$,[21] the surface structure factor (1.9) is predicted to be linear in $q_\perp$. The dependence of the slope on the areal density n_0 of flux lines is, however, different in two regimes. For $q_\perp<1/L$ we find $S_{2T}(q_\perp,L)\sim q_\perp/n_0$, while for $q_\perp>q_\perp^*$, $S_{2T}(q_\perp,L)\sim q_\perp/n_0^{1/2}$. The latter behavior is consistent with experiments. The experiments are carried out on slabs which are typically of 1-mm extent and 5–30 μm thickness. Due to the finite size of the decoration images only information on the structure function for $q_\perp\geq 0.4$ μm can typically be extracted from the experiments that are therefore unable to probe the range $q_\perp<1/L$. In fact the experimental structure factors appear to level out in the small-$q_\perp$ range.[22] One can therefore conclude that the patterns probed by decorations are indeed representative of bulk behavior. Only the asymptotic behavior at very

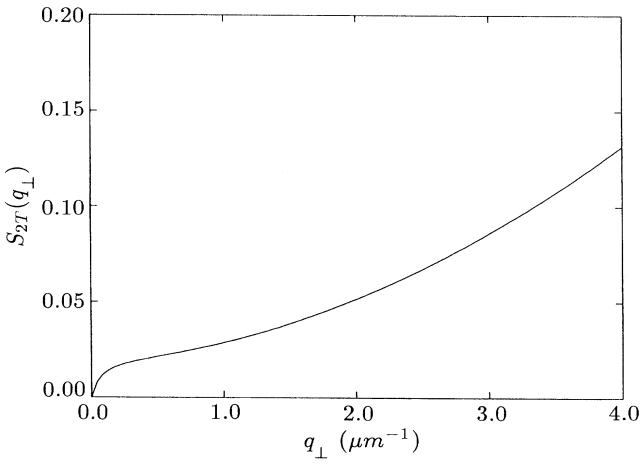

FIG. 1. Thermal contribution to the surface structure function, as given in Eq. (1.8), for $H=8$ G (for this value of the field the first maximum of $S_2(q_\perp)$ is at $q_\perp\simeq 4.26$ μm^{-1}), $T=88$ K, $\lambda_{ab}=0.3$ μm, $\gamma=55$, and $L=25$ μm. Here $B_3(0)$ was treated as a parameter determined by fitting our results to the small wave-vector part of the data of Ref. 22, as discussed in Sec. III.

long length scales is dominated by surface effects. These large length scales have not, however, been accessible in experiments.

In Sec. II we present a simple-model hydrodynamic free energy for a flux-line liquid in a finite-size superconductor sample that properly incorporates the boundary conditions at the superconductor-vacuum surface. This free energy is used to evaluate the thermal part of the structure function at the sample's surface. In Sec. III we introduce disorder in the hydrodynamical treatment and discuss its effect on the translational correlations at the sample surface. The comparison with experiments is discussed in Sec. IV. In Appendix A we present the results for the full three-dimensional structure function defined in Eq. (1.1).

II. HYDRODYNAMIC FREE ENERGY AND SURFACE STRUCTURE FUNCTION

The pair interaction between flux lines in a finite-size superconductor sample has been derived before in the London approximation for both isotropic[23] and anisotropic[24,19] superconductors. In Ref. 19 we calculated the magnetic energy of the flux-line array in a semi-infinite sample of anisotropic CuO_2 superconductor occupying the half space $z<0$, where the z direction is the $\hat{\mathbf{c}}$ axis of the material and the field is applied along the $\hat{\mathbf{c}}$ axis. The calculation of the energy for a superconducting slab of thickness L can be carried out along the same lines. In general, the magnetic energy from the stray fields in the region outside the superconductor can always be rewritten as a surface contribution to the pair interaction between flux lines that decays exponentially with the distance from the interface. For straight lines the pair interaction behaves as discussed by Pearl and it decays as $1/r_\perp$ at large distances at the superconductor's surfaces. Following Ref. 19, this pair interaction can then be used to obtain the coarse-grained hydrodynamic free energy. The presence of the superconducting-vacuum interface modifies the compressional and tilt elastic constants of the flux-line array. In addition to the familiar nonlocality of the elastic constants associated with the range of the repulsive interaction between flux-line elements, the presence of the interface introduces additional nonlocalities in the z direction. The corresponding surface contributions to the elastic constants depend exponentially on the distance of the deformed flux volume from the interface. The surface contribution to the wave-vector-dependent bulk modulus diverges as $1/q_\perp$ at small wave vectors, as expected for particles interacting via a $1/r_\perp$ potential in two dimensions. The surface contribution to the tilt modulus is negative and finite in the small wave-vector limit.

Instead of using this general hydrodynamic free energy, here we propose a much simpler model free energy that neglects all nonlocalities in the z direction, other than the presence of the superconductor-vacuum boundaries. For clarity we consider in this section the case of a clean superconductor. The effect of weak impurity disorder on the translational correlation functions of a finite-thickness flux-line liquid will be discussed in the next section. The flux liquid free energy is then written as the sum of bulk and surface contributions,

$$F=F_B+F_S\ , \tag{2.1}$$

where F_B is the usual hydrodynamic free energy for a bulk flux-line liquid. It includes terms quadratic in the hydrodynamic fields, which are the density field defined in (1.2) and a tilt field, defined as,

$$t(\mathbf{r}_\perp,z)=\sum_{i=1}^{N}\frac{\partial \mathbf{r}_i}{\partial z}\delta(\mathbf{r}_\perp-\mathbf{r}_i(z))\ . \tag{2.2}$$

The bulk free energy is given in Ref. 1,

$$F_B=\frac{1}{2n_0^2A}\sum_{\mathbf{q}_\perp}\int_0^L dz\{B_3(q_\perp)|\delta n(\mathbf{q}_\perp,z)|^2 +K(q_\perp)|\mathbf{t}(\mathbf{q}_\perp,z)|^2\}\ . \tag{2.3}$$

Since we are allowing for in-plane nonlocality of the elastic constants, we have written the free energy in terms of the Fourier components of the hydrodynamic densities. There are two surface contributions to the free energy,

$$F_S=\frac{1}{2n_0^2A}\sum_{\mathbf{q}_\perp}\{B_2(q_\perp)|\delta n_v(\mathbf{q}_\perp,z=0)|^2 +B_2(q_\perp)|\delta n_v(\mathbf{q}_\perp,z=L)|^2\}\ , \tag{2.4}$$

where $B_2(q_\perp)$ is the surface contribution to the bulk modulus obtained in Ref. 19 and given by

$$B_2(q_\perp)=\frac{B^2}{4\pi q_\perp}\frac{1}{(1+q_\perp^2\lambda_{ab}^2)^{3/2}(q_\perp\lambda_{ab}+\sqrt{1+q_\perp^2\lambda_{ab}^2})}\ . \tag{2.5}$$

For $q_\perp\lambda_{ab}\ll 1$ it is well approximated by the compressional modulus of a two-dimensional fluid of particles interacting via a $1/\mathbf{r}_\perp$ potential, $B_2(q_\perp)\simeq B^2/(4\pi q_\perp)$.

Statistical averages over vortex line configurations have to be carried out over the free energy (2.1) with the constraint that flux lines cannot start nor stop inside the medium,

$$\partial_z\delta n(\mathbf{q}_\perp,z)+i\mathbf{q}_\perp\cdot\mathbf{t}(\mathbf{q}_\perp,z)=0\ . \tag{2.6}$$

It is convenient to separate $\mathbf{t}(\mathbf{q}_\perp,z)$ in its longitudinal and transverse parts, $\mathbf{t}=\hat{\mathbf{q}}_\perp t_L+\hat{\mathbf{z}}\times\hat{\mathbf{q}}_\perp t_T$, with $t_L=\hat{\mathbf{q}}_\perp\cdot\mathbf{t}$ and $t_T=(\hat{\mathbf{z}}\times\hat{\mathbf{q}}_\perp)\cdot\mathbf{t}$. As a result of the constraint (2.6), the density and the longitudinal part of the tangent field are not independent hydrodynamic variables. In fact they can both be expressed in terms of a "vector potential" $\mathbf{u}(\mathbf{q}_\perp,z)$, which plays the role of a two-dimensional displacement field for the flux-line liquid,

$$\begin{aligned}\delta n(\mathbf{q}_\perp,z)&=-n_0 i\mathbf{q}_\perp\cdot\mathbf{u}(\mathbf{q}_\perp,z)\ ,\\ t_L(\mathbf{q}_\perp,z)&=n_0\partial_z\hat{\mathbf{q}}_\perp\cdot\mathbf{u}(\mathbf{q}_\perp,z)\ .\end{aligned} \tag{2.7}$$

The transverse degrees of freedom t_T are decoupled from the longitudinal ones. Since in this paper we are only interested in calculating correlation functions of density fluctuations, we only need to consider the longitudinal part of the free energy. This can be expressed entirely in terms of $u_L(\mathbf{q}_\perp,z)=\hat{\mathbf{q}}_\perp\cdot\mathbf{u}(\mathbf{q}_\perp,z)$ so that the constraint (2.6) is automatically satisfied, with the result,

$$F^{(L)}=\frac{1}{2A}\sum_{\mathbf{q}_\perp}\int_0^L\left\{K(q_\perp)\left|\frac{du_L}{dz}\right|^2+B_3(q_\perp)q_\perp^2|u_L(\mathbf{q}_\perp,z)|^2+[\delta(z)+\delta(z-L)]B_2(q_\perp)q_\perp^2|u_L(\mathbf{q}_\perp,z)|^2\right\}. \tag{2.8}$$

The tilt energy provides the coupling between bulk and surface terms. The model free energy of Eq. (2.8) has the same structure of model free energies used to study surface phase transitions, particularly in the context of wetting.[25] The longitudinal component of the vector potential takes the place of the order parameter and the presence of interfaces introduces spatial inhomogeneities in the order parameter.

One could now proceed directly to evaluate correlation functions of the field u_L by taking statistical averages with the free energy (2.8). The two-dimensional structure factor of the flux-line tips at the top surface is simply given by $S_{2T}(q_\perp)=n_0q_\perp^2\langle|u_L(\mathbf{q}_\perp,L)|^2\rangle$, where the angular brackets denote the statistical average over the free energy (2.8). Since the free energy is quadratic in the fields, these correlation functions can be calculated exactly. On the other hand, due to the coupling of the field at the surface to the field in the bulk of the sample the calculation is somewhat lengthy and tedious. A much simpler way to obtain the same results is to use linear response theory. Let us apply a spatially inhomogeneous surface pressure $\delta p(\mathbf{r}_\perp)$ at $z=L$ and consider the linear response of the system to this perturbation. The surface pressure couples to the density and the free energy of the corresponding perturbation is given by

$$\delta F_p=\frac{1}{n_0}\int d\mathbf{r}_\perp\delta p(\mathbf{r}_\perp)\delta n(\mathbf{r}_\perp,L)=-\frac{1}{A}\sum_{\mathbf{q}_\perp}iq_\perp\delta p(\mathbf{q}_\perp)u_L(\mathbf{q}_\perp,L). \tag{2.9}$$

The response to this perturbation is a nonvanishing average displacement, $\langle u_L(\mathbf{q}_\perp,z)\rangle_p$, that can be determined by minimizing the total free energy, that is, by requiring,

$$\frac{\delta[F^{(L)}+\delta F_p]}{\delta u_L(\mathbf{q}_\perp,z)}=0. \tag{2.10}$$

The minimization of the total free energy yields an equation for the displacement field in the bulk of the sample,

$$-K\partial_z^2\langle u_L(z)\rangle_p+q_\perp^2B_3\langle u_L(z)\rangle_p=0, \tag{2.11}$$

for $z\neq0$, L, and boundary conditions for the displacement field at the superconductor-vacuum surfaces,

$$K[\partial_z\langle u_L\rangle_p]_{z=L}+q_\perp^2B_2\langle u_L(L)\rangle_p-iq_\perp\delta p=0, \tag{2.12}$$

$$-K[\partial_z\langle u_L\rangle_p]_{z=0}+\mathbf{q}_\perp^2B_2\langle u_L(0)\rangle_p=0. \tag{2.13}$$

By solving Eq. (2.11) with the boundary conditions (2.12) and (2.13) we obtain,

$$\langle u_L(\mathbf{q}_\perp,z)\rangle_p=A_1e^{-z/\xi_\parallel}+A_2e^{z/\xi_\parallel}, \tag{2.14}$$

where $\xi_\parallel(q_\perp)$ is the correlation length defined in Eq. (1.7) and

$$A_1=\frac{i}{2q_\perp}\frac{B_3\xi_\parallel-B_2}{[B_3^2\xi_\parallel^2+B_2^2]\sinh(L/\xi_\parallel)+2B_3\xi_\parallel B_2\cosh(L/\xi_\parallel)}\delta p(\mathbf{q}_\perp),$$
$$A_2=\frac{i}{2q_\perp}\frac{B_3\xi_\parallel+B_2}{[B_3^2\xi_\parallel^2+B_2^2]\sinh(L/\xi_\parallel)+2B_3\xi_\parallel B_2\cosh(L/\xi_\parallel)}\delta p(\mathbf{q}_\perp). \tag{2.15}$$

The surface displacement is then given by,

$$\langle u_L(\mathbf{q}_\perp,L)\rangle_p=i\frac{\delta p(\mathbf{q}_\perp)}{q_\perp}\frac{1}{B_2(q_\perp)+B_3(q_\perp)\xi_\parallel(q_\perp)F(L/\xi_\parallel)}, \tag{2.16}$$

where $F(L/\xi_\parallel)$ is the crossover function given in Eq. (1.11). As expected, the response to the applied pressure is linear in the perturbation. The corresponding linear response function defined as

$$\chi_T(q_\perp,L)=\frac{\delta n(\mathbf{q}_\perp,L)}{\delta p(\mathbf{q}_\perp)}=\frac{-iq_\perp n_0\langle u_L(\mathbf{q}_\perp,L)\rangle_p}{\delta p(\mathbf{q}_\perp)}, \tag{2.17}$$

is the wave-vector-dependent surface isothermal compressibility, which is in turn the reciprocal of the two-dimensional surface bulk modulus, $B_2^{\rm eff}(q_\perp,L)=1/\chi(q_\perp,L)$. The denominator of Eq. (2.16) is then the effective surface bulk modulus given in Eq. (1.10). Finally, the surface structure factor is given by Eq. (1.9).

III. WEAK DISORDER

The effect of weak disorder both in the bulk of the sample and at the superconductor-vacuum interfaces can be

modeled in a standard way in terms of a random potential that couples to the density field. In general, surface disorder may include surface roughness and therefore differ considerably from impurity disorder in bulk. We therefore model bulk and surface disorder separately by adding to the free energy given in Eq. (2.8) two terms,

$$\delta F_D=\int d\mathbf{r}_\perp\int_0^L\{V_b(\mathbf{r}_\perp,z)\delta n(\mathbf{r}_\perp,z) +[\delta(z)+\delta(z-L)]V_s(\mathbf{r}_\perp)\delta n(\mathbf{r}_\perp,z)\}\ , \tag{3.1}$$

where the random potentials $V_b(\mathbf{r}_\perp,z)$ and $V_s(\mathbf{r}_\perp)$ represent the effect of random impurities and small-scale inhomogeneities in the bulk and at the surface, respectively. If the defects are randomly distributed, as for instance in the case of oxygen vacancies, we expect that the quenched fluctuations in the impurity potentials will obey,

$$\overline{V_b(\mathbf{r}_\perp,z)V_b(\mathbf{r}'_\perp z')}=\Delta_b\delta(\mathbf{r}_\perp-\mathbf{r}'_\perp)\delta(z-z')\ ,$$
$$\overline{V_s(\mathbf{r}_\perp)V_s(\mathbf{r}'_\perp)}=\Delta_s\delta(\mathbf{r}_\perp-\mathbf{r}'_\perp)\ , \tag{3.2}$$

with $\overline{V_b(\mathbf{r}_\perp,z)}=0$ and $\overline{V_s(\mathbf{r}_\perp)}=0$.

It was shown by Nelson and Le Doussal[15] that in bulk flux-line liquids a hydrodynamic treatment of weak bulk disorder produces "Lorentzian squared" correction to the hydrodynamic result for the structure factor, given by

$$S_{bd}(q_\perp,q_z)=n_0\Delta_b\left[\frac{n_0q_\perp^2}{q_\perp^2B_3+q_z^2K}\right]^2\ , \tag{3.3}$$

or, by inverting the q_z transform,

$$S_{bd}(q_\perp,z_1-z_2)=n_0\Delta_b\left[\frac{n_0}{B_3(q_\perp)\xi_\parallel(q_\perp)}\right]^2 \times[\xi_\parallel(q_\perp)+|z_1-z_2|]e^{-|z_1-z_2|/\xi_\parallel}\ . \tag{3.4}$$

The contribution from weak disorder to two-dimensional density correlations in a constant-z cross section of bulk, is then obtained from (3.4) by letting $z_1=z_2$,

$$S_{2bd}(q_\perp)=\frac{n_0^3\Delta_b\xi_\parallel(q_\perp)}{[B_3(q_\perp)\xi_\parallel(q_\perp)]^2}\ . \tag{3.5}$$

Notice that this contribution to the two-dimensional structure factor of a cross section of flux-line liquid also vanishes linearly with $q_\perp$ at small wave vectors.

To evaluate the two-dimensional structure factor of flux-line tips at the surface of a slab of type-II superconductor in a field, we proceed as in Sec. II. The total free energy $F^{(L)}+F_D$ of the flux-line liquid consists now of the sum of Eqs. (2.8) and (3.1). To this we add the surface perturbation given in (2.9) and evaluate the response of the system by minimizing the total free energy. As in Sec. II we obtain an equation for the displacement field in the bulk of the sample,

$$-K\partial_z^2\langle u_L(z)\rangle_p+q_\perp^2B_3\langle u_L(z)\rangle_p-iq_\perp n_0V_b(\mathbf{q}_\perp,z)=0\ , \tag{3.6}$$

for $z\neq0$, L, and boundary conditions for the displacement field at the superconductor-vacuum surfaces,

$$K[\partial_z\langle u_L\rangle_p]_{z=L}+q_\perp^2B_2\langle u_L(L)\rangle_p -iq_\perp n_0V_s(\mathbf{q}_\perp)-iq_\perp\delta p=0\ , \tag{3.7}$$

$$-K[\partial_z\langle u_L\rangle_p]_{z=0}+q_\perp^2B_2\langle u_L(z=0)\rangle_p -iq_\perp n_0V_s(\mathbf{q}_\perp)=0\ . \tag{3.8}$$

The solution of Eq. (3.6) with the boundary conditions (3.7) and (3.8) is given by,

$$\langle u_L(\mathbf{q}_\perp,z)\rangle_p=A'_1e^{-z/\xi_\parallel}+A'_2e^{z/\xi_\parallel}-\frac{in_0\xi_\parallel}{K}\int_0^z dz'\cosh[(z-z')/\xi_\parallel]V_b(\mathbf{q}_\perp,z')\ , \tag{3.9}$$

with

$$A'_1=\frac{i}{2q_\perp}\frac{1}{[B_3^2\xi_\parallel^2+B_2^2]\sinh(L/\xi_\parallel)+2B_3\xi_\parallel B_2\cosh(L/\xi_\parallel)} \times\left\{[B_3\xi_\parallel-B_2]\delta p(\mathbf{q}_\perp)+n_0V_s(\mathbf{q}_\perp)[(B_3\xi_\parallel-B_2)+(B_3\xi_\parallel+B_2)e^{L/\xi_\parallel}] +n_0(B_3\xi_\parallel-B_2)\int_0^L dz\ V_b(\mathbf{q}_\perp,z)\left[\cosh\left[\frac{L-z}{\xi_\parallel}\right]+\frac{B_2}{B_3\xi_\parallel}\sinh\left[\frac{L-z}{\xi_\parallel}\right]\right]\right\}\ , \tag{3.10}$$

$$A'_2=\frac{i}{2q_\perp}\frac{1}{[B_3^2\xi_\parallel^2+B_2^2]\sinh(L/\xi_\parallel)+2B_3\xi_\parallel B_2\cosh(L/\xi_\parallel)} \times\left\{[B_3\xi_\parallel+B_2]\delta p(\mathbf{q}_\perp)+n_0V_s(\mathbf{q}_\perp)[(B_3\xi_\parallel+B_2)+(B_3\xi_\parallel-B_2)e^{-L/\xi_\parallel}] +n_0(B_3\xi_\parallel+B_2)\int_0^L dz\ V_b(\mathbf{q}_\perp,z)\left[\cosh\left[\frac{L-z}{\xi_\parallel}\right]+\frac{B_2}{B_3\xi_\parallel}\sinh\left[\frac{L-z}{\xi_\parallel}\right]\right]\right\}\ . \tag{3.11}$$

The solution (3.9) depends explicitly on the impurity potentials V_b and V_s and represents the longitudinal displacement field for a given realization of the disorder. In the presence of quenched disorder the fluctuation-dissipation theorem no longer holds and one cannot simply identify the ratio of the mean displacement $\overline{\langle u_L(\mathbf{q}_\perp,z)\rangle_p}$ to the perturbation $\delta p(\mathbf{q}_\perp)$ with the system's compressibility. In fact the mean displacement in the presence of weak disorder is simply equal to that given in (2.14) for a clean superconductor. This is because the terms linear in the impurity potentials in Eq. (3.9) vanish when averaged over the quenched disorder and $\overline{A_1'}=A_1$ and $\overline{A_2'}=A_2$. One then needs to calculate directly the correlation function of the fluctuations as defined in Eq. (1.4), or, in terms of the linear response, $\langle u_L(\mathbf{q}_\perp,L)\rangle_p$,

$$S(\mathbf{q}_\perp,z_1,z_2)=n_0\mathbf{q}_\perp^2[\overline{\langle u_L(\mathbf{q}_\perp,z_1)\rangle_p\langle u_L(-\mathbf{q}_\perp,z_2)\rangle}-\overline{\langle u_L(\mathbf{q}_\perp,z_1)\rangle_p}\,\overline{\langle u_L(-\mathbf{q}_\perp,z_2)\rangle_p}] \ . \tag{3.12}$$

After some algebra, one finds that the two-dimensional structure factor at the surface $z=L$ of the slab, $S_2(q_\perp,L)=S(q_\perp,z_1=L,z_2=L)$, can be written as the sum of three contributions,

$$S_2(q_\perp,L)=S_{2T}(q_\perp,L)+S_{2db}(q_\perp,L)+S_{2sd}(q_\perp,L) \ , \tag{3.13}$$

where $S_{2T}(q_\perp,L)$ is the contribution from thermal fluctuations that was already obtained in Sec. II,

$$S_{2T}(q_\perp,L)=\frac{n_0k_BT}{B_2^{\rm eff}(q_\perp,L)} \ , \tag{3.14}$$

with $B_2^{\rm eff}(q_\perp,L)$ the surface bulk modulus given in Eq. (1.10). The other two terms in Eq. (3.13) represent the contributions from bulk and surface disorder, respectively. They are given by

$$S_{2bd}(q_\perp,L)=\frac{n_0^3\Delta_b\xi_\parallel}{2[B_2^{\rm eff}(q_\perp,L)]^2}\frac{1}{[B_2+B_3\xi_\parallel\coth(L/\xi_\parallel)]^2} \times\left\{[B_3^2\xi_\parallel^2+B_2^2]\coth(L/\xi_\parallel)+2B_2B_3\xi_\parallel+[B_3^2\xi_\parallel^2-B_2^2]\frac{L/\xi_\parallel}{\sinh^2(L/\xi_\parallel)}\right\} , \tag{3.15}$$

and

$$S_{2sd}(q_\perp,L)=\frac{n_0^3\Delta_s}{[B_2^{\rm eff}(q_\perp,L)]^2}\left\{1+\frac{B_3^2\xi_\parallel^2/\sinh^2(L/\xi_\parallel)}{[B_2+B_3\xi_\parallel\coth(L/\xi_\parallel)]^2}\right\} . \tag{3.16}$$

While these expressions appear rather complicated, one can show that for all $q_\perp$ of interest here the terms inside curly brackets in Eqs. (3.15) and (3.16) are of order one.

IV. DISCUSSION

The surface structure factors extracted from the analysis of the low-field decoration experiments carried out by the AT&T group show clearly a large peak at $q_\perp=4\pi/(\sqrt{3}a_0)$, where $a_0=(2/\sqrt{3}a_0)^{1/2}$ is the nearest-neighbor vortex spacing in the triangular Abrikosov lattice.[9] At smaller wave vectors the structure functions obtained at different applied fields all decrease linearly with wave vector according to $S_2(q_\perp,L)\sim q_\perp/n_0^{1/2}$.[9] At the smallest wave vectors probed in the experiments, the decay of the structure functions seems to be leveling out.[22] This behavior is most apparent in the experiments at the lowest fields.

To discuss the comparison of our results with these experimental findings, it is useful to consider some limiting forms of the expressions obtained in Secs. II and III.

When the sample thickness L is large compared to the correlation length $\xi_\parallel$ the expressions given in Sec. II and III for the surface structure factors reduce to those for the two-dimensional structure factors at the surface of a semi-infinite sample of type-II superconductor. In this limit, $L\gg\xi_\parallel$ or $q_\perp\gg q_\perp^*$, the crossover function given in Eq. (1.11) is $F(L/\xi_\parallel)\approx 1$ and we find

$$S_{2T}(q_\perp,L)\simeq\frac{n_0k_BT}{B_2+B_3\xi_\parallel}\sim q_\perp \ , \tag{4.1}$$

$$S_{2bd}(q_\perp,L)\simeq\frac{n_0^3\Delta_b\xi_\parallel}{2[B_2+B_3\xi_\parallel]^2}\sim q_\perp \ , \tag{4.2}$$

$$S_{2sd}(q_\perp,L)\simeq\frac{n_0^3\Delta_s}{[B_2+B_3\xi_\parallel]^2}\sim q_\perp^2 \ . \tag{4.3}$$

In this limit all contributions to the surface structure factor are determined by an effective bulk modulus $B_2+B_3\xi_\parallel\sim B_3(1+\sqrt{K/B_3})/q_\perp$, where we approximated $B_2\sim B_3/q_\perp$.[19] As indicated in Eqs. (4.1)–(4.3), while both the contributions to the structure factor from thermal fluctuations and from bulk disorder are linear in $q_\perp$ in this regime, the contribution from surface disorder is proportional to $q_\perp^2$. We argue below that the linear dependence of the surface structure factor on $q_\perp$ observed in the decoration experiments by the AT&T group[9,22] probably corresponds to this regime. If our interpretation is correct, our results indicate that surface roughness does not play an important role in these experiments.

In the opposite limit, $L\ll\xi_\parallel$, the flux lines are essentially straight over the entire thickness of the sample. The crossover function (1.11) becomes $F(L/\xi_\parallel)\approx(B_2+B_3L)/B_3\xi_\parallel$ and the various contributions to the

surface structure factor are given by

$$S_{2T}(q_\perp,L)\simeq\frac{n_0k_BT}{2B_2+B_3L}\ , \tag{4.4}$$

$$S_{2bd}(q_\perp,L)\simeq\frac{n_0^3\Delta_bL}{2[2B_2+B_3L]^2}\ , \tag{4.5}$$

$$S_{2sd}(q_\perp,L)\simeq\frac{2n_0^3\Delta_s}{[2B_2+B_3L]^2}\ . \tag{4.6}$$

When $q_\perp\to0$, $B_2\sim q_\perp^{-1}$ while $B_3\sim q_\perp^0$, and B_2 always dominates in the denominator of Eqs. (4.4)–(4.6), yielding,

$$\lim_{q_\perp\to0}S_{2T}(q_\perp,L)\simeq\frac{n_0k_BT}{2B_2}\sim q_\perp\ , \tag{4.7}$$

$$\lim_{q_\perp\to0}S_{2bd}(q_\perp,L)\simeq\frac{n_0^3\Delta_bL}{4B_2^2}\sim q_\perp^2\ , \tag{4.8}$$

$$\lim_{q_\perp\to0}S_{2sbd}(q_\perp,L)\simeq\frac{n_0^3\Delta_s}{2B_2^2}\sim q_\perp^2\ . \tag{4.9}$$

If $B_2\sim B_3/q_\perp$, the above limiting forms apply in the entire range $q_\perp\ll1/L$. Finally, if the ratio K/B_3 is large enough so that there is a nonvanishing range of wave vectors where $1/L<q_\perp<q_\perp^*$, in this range the surface structure factors level out to a constant value, given by

$$S_{2T}(q_\perp,L)\simeq\frac{n_0k_BT}{LB_3}\ , \tag{4.10}$$

$$S_{2bd}(q_\perp,L)\simeq\frac{n_0^3\Delta_b}{LB_3^2}\ , \tag{4.11}$$

$$S_{2sd}(q_\perp,L)\simeq\frac{2n_0^3\Delta_s}{(LB_3)^2}\ . \tag{4.12}$$

We remark that if one evaluates the surface structure factors for a finite-thickness superconducting slab using free boundary conditions for the flux lines at the sample surfaces, one finds that in the limit $q_\perp\to0$ the various contributions to $S_2(q_\perp,L)$ have precisely the sample-size-dependent constant values given in (4.10)–(4.12). In fact for all values of $q_\perp$ where our hydrodynamic theory is relevant, the expressions for $S_2(q_\perp,L)$ for the case of free boundary conditions on the flux lines are obtained from those given here by setting $B_2=0$. The precise nature of the boundary conditions only affects the very small $q_\perp$ behavior of the correlation functions.

We conclude by discussing in some detail the comparison of our findings with the experimental structure factors obtained by Murray and collaborators from low-field decoration images.[9,22] The fields in these experiments are in the range 8–50 G, corresponding to flux-line areal densities of 0.4–2.5 μm^{-2}. The smallest wave vectors at which one can construct a structure function from the decoration images is ~0.4 μm^{-1}. The long-wavelength tail of $S_2(q_\perp)$ is found to fit a $q_\perp/n_0^{1/2}$ in an intermediate range of wave vectors. The slope of $S_2(q_\perp)$ in this linear region is typically $\sim5\times10^{-3}-10^{-2}$ μm. At the smallest wave vectors where data are available $S_2(q_\perp)$ appears to be leveling out to a constant value ~0.02, almost independent of the applied field.

Our model predicts a linear decrease of $S_{2T}(q_\perp)$ with $q_\perp$ in the limit $q_\perp\to0$. The corresponding slope is determined by $B_2\sim n_0^2\phi_0^2/(4\pi q_\perp)$ according to Eq. (4.7). One finds $S_{2T}(q_\perp)\sim2\times10^{-6}$ $\mu m^{-1}K^{-1}(T/n_0)q_\perp$. Using $T\sim88$ K and $n_0\sim1$ μm^{-2}, we obtain $S_{2T}(q_\perp)\sim2\times10^{-5}$ μm $q_\perp$, a slope over two orders of magnitude smaller than observed in experiments. In addition the dependence of the slope on the density is not of the form obtained in the experimental fit. Finally, in the limit $q_\perp\to0$, both contributions to the structure functions from weak disorder vanish as $q_\perp^2$. All of this is consistent with the expectation that this asymptotic long wavelength regime is never probed in the experiments.

If the ratio $\sqrt{K/B_3}\le1$, then for all wave vectors accessible to experiments $\xi_\parallel<L$ and the various contributions to the surface structure function are given by Eqs. (4.1)–(4.3). Again we have a linear dependence of $S_{2T}(q_\perp)$ on $q_\perp$, but with a slope even smaller than in the asymptotic $q_\perp\to0$ case discussed above. A similar estimate can be carried our for the contribution from bulk disorder. In this case the size of the linear slope is determined by Δ_b. If the pinning is by isolated O_2 vacancies, we can estimate $\Delta_b\sim U_0^2\xi_{ab}$, with $U_0\sim5K$ a typical pinning energy barrier. The corresponding linear slope is then even smaller than for the thermal part of the correlation function.

Our results are qualitatively consistent with the experimental findings if $\sqrt{K/B_3}\gg1$. In this case we predict a crossover from the linear dependence of $S_2(q_\perp)$ on $q_\perp$ described by Eqs. (4.1) and (4.2) for $q_\perp>q_\perp^*$ to the sample-size-dependent constant values given by Eqs. (4.10) and (4.11). On the other hand, the predicted size of the constant value of $S_2(q_\perp)$ for $q_\perp\le q_\perp^*$ and the linear slope at larger wave vectors are more than an order of magnitude smaller than from experiments, even when we take into account the in-plane nonlocality of the elastic constants. We can in turn try to fit our results to experiments to extract experimental values for the elastic constants. For instance, in Fig. 1, by requiring $S_2(q_\perp\ge1/L)\sim n_0k_BT/(B_3^{\rm exp}L)\sim0.02$ for $H=8$ G, we find $B_3^{\rm exp}/k_B\sim70K$ μm^{-3} for $L\sim10$ μm. This value is about 500 times smaller than $B_3(0)=B^2/4\pi$, nor can the in-plane nonlocality of B_3 account for the difference. We can then extract a value of the tilt modulus K by fitting the slope in the linear region, $S_2(q_\perp\ge q_\perp^*)\sim(n_0k_BT/\sqrt{K^{\rm exp}B_3^{\rm exp}})q_\perp\sim0.02$ μm $q_\perp$. We find $K^{\rm exp}/K_B\sim4.4\times10^4k$ μm^{-3}, a value not inconsistent with the theoretical value for $K(0)$. The corresponding crossover wave vector is $q_\perp^*=(1/L)\sqrt{K^{\rm exp}/B_3^{\rm exp}}\sim1$ μm^{-1}. A mechanism that can account quantitatively for the very small value of B_3 could be the strong downward renormalization of the compressional modulus that was predicted by Nelson and Le Doussal at low density.[15]

In conclusion, our work indicates clearly that, while the decay of translational correlations at very long wavelengths ($q_\perp\to0$) is indeed governed by surface properties and finite-size effects, the correlation functions extracted

from the decoration experiments are in fact representative of bulk behavior. More data at small wave vectors and low fields with a detailed analysis of such data are, however, needed for a quantitative comparison.

ACKNOWLEDGMENTS

Work by M.C.M. was supported by the NSF through Grant No. DMR-91-12330. D.R.N. acknowledges support from the NSF through the Harvard Materials Research Laboratory and through Grant No. DMR-91-15491. We are grateful to C. A. Murray and D. Grier for sharing with us experimental results prior to publication.

APPENDIX A: THREE-DIMENSIONAL STRUCTURE FUNCTION

In this appendix we discuss the full three-dimensional structure function given in Eq. (1.1). We only sketch the derivation of the thermal part of this correlation function, $S_T(q_\perp,z,z_0)$. This derivation is instructive as an example of how to evaluate correlation functions directly by taking statistical averages with the free energy (2.8) rather than by using linear response theory.

It is convenient to expand the displacement field $u_L(\mathbf{q}_\perp,z)$ in a Fourier series,

$$u_L(\mathbf{q}_\perp,z)=\frac{1}{L}\left\{u_0(\mathbf{q}_\perp)+2\sum_{p=1}^{\infty}[u_p(\mathbf{q}_\perp)\cos(p\pi z/L)+v_p(\mathbf{q}_\perp)\sin(p\pi z/L)]\right\} . \tag{A1}$$

The free energy (2.8) is immediately rewritten in terms of the Fourier amplitudes of the displacement field, with the result,

$$F^L=\frac{1}{2AL^2}\sum_{\mathbf{q}_\perp}\left\{\sum_{p=-\infty}^{\infty}\alpha_p(q_\perp)(|u_p(\mathbf{q}_\perp)|^2+|v_p(\mathbf{q}_\perp)|^2)+\frac{B_2}{L}q_\perp^2\left|\sum_{p=-\infty}^{\infty}u_p(\mathbf{q}_\perp)\right|^2+\frac{B_2}{L}q_\perp^2\left|\sum_{p=-\infty}^{\infty}(-1)^p u_p(\mathbf{q}_\perp)\right|^2\right\} , \tag{A2}$$

with

$$\alpha_p(q_\perp)=K\left[\frac{p\pi}{L}\right]^2+B_3q_\perp^2 , \tag{A3}$$

where $v_0(\mathbf{q}_\perp)=0$ and we used that $u_p(-\mathbf{q}_\perp)=u_p(\mathbf{q}_\perp)$ and $v_p(-\mathbf{q}_\perp)=-v_p(\mathbf{q}_\perp)$. Using Eq. (2.7), the thermal part of the three-dimensional structure function can be written in terms of the longitudinal displacement field,

$$S_T(q_\perp,z_1,z_2)=n_0q_\perp^2\langle u_L(\mathbf{q}_\perp,z_1)u_L(-\mathbf{q}_\perp,z_2)\rangle . \tag{A4}$$

By inserting Eq. (A1) into Eq. (A4) we obtain

$$S_T(q_T,z_1,z_2)=\frac{n_0q_\perp^2}{L^2}\sum_{p=-\infty}^{\infty}\sum_{p'=-\infty}^{\infty}\{\langle u_p(q_\perp)u_{p'}^*(q_\perp)\rangle\cos(p\pi z_1/L)\cos(p'\pi z_2/L)+\langle v_p(q_\perp)v_{p'}^*(q_\perp)\rangle\sin(p\pi z_1/L)\sin(p'\pi z_2/L)\} . \tag{A5}$$

The correlation functions of the Fourier amplitudes of the displacement field can be calculated by using standard tricks to deal with coupled Gaussian integrals. The result is

$$\langle v_p(\mathbf{q}_\perp)v_{p'}(-\mathbf{q}_\perp)\rangle=\delta_{p,p'}\frac{Lk_BT}{\alpha_p(q_\perp)} , \tag{A6}$$

and

$$\langle u_p(\mathbf{q}_\perp)u_{p'}(-\mathbf{q}_\perp)\rangle=\delta_{p,p'}\frac{Lk_BT}{\alpha_p(q_\perp)}-\frac{k_BTB_2q_\perp^2}{\alpha_p\alpha_{p'}}\frac{1}{(1+B_2q_\perp^2S_o)^2-(B_2q_\perp^2S_e)^2}\times\{(1+B_2q_\perp^2S_o)[1+(-1)^{p+p'}]-B_2q_\perp^2S_e[(-1)^p+(-1)^{p'}]\} . \tag{A7}$$

The quantities denoted by S_o and S_e are special cases of more general sums that will be needed below. These are,

$$\sum_o(q_\perp,z)=\frac{1}{L}\sum_{p=-\infty}^{\infty}\frac{\cos(p\pi z/L)}{\alpha_p(q_\perp)}=\frac{1}{B_3\xi_\parallel q_\perp^2}\frac{\cosh[(z-L)/\xi_\parallel]}{\sinh(L/\xi_\parallel)} , \tag{A8}$$

$$\sum_e(q_\perp,z)=\frac{1}{L}\sum_{p=-\infty}^{\infty}\frac{(-1)^p\cos(p\pi z/L)}{\alpha_p(q_\perp)}=\frac{1}{B_3\xi_\parallel q_\perp^2}\frac{\cosh(z/\xi_\parallel)}{\sinh(L/\xi_\parallel)} , \tag{A9}$$

with $\xi_\parallel(q_\perp)$ the correlation length given in Eq. (1.7). The quantities S_o and S_e are given by the values of the above sums

at $z=0$, i.e., $S_o=\sum_o(q_\perp,0)$ and $S_e=\sum_e(q_\perp,0)$.

Finally, by inserting Eqs. (A7) and (A6) into Eq. (A5), one obtains

$$S_T(q_\perp,z_1,z_2)=\frac{n_0k_BT}{B_3\xi_\parallel}\left\{\frac{\cosh[(z_1-z_2-L)/\xi_\parallel]}{\sinh(L/\xi_\parallel)}-\frac{B_2}{B_2+B_3\xi_\parallel F(L/\xi_\parallel)}\right.$$
$$\left.\times\left[\frac{\cosh[(z_1+z_2-L)/\xi_\parallel]}{\sinh(L/\xi_\parallel)}+\frac{B_3\xi_\parallel}{B_2+B_3\xi_\parallel\coth(L/\xi_\parallel)}\frac{\cosh[(z_1-z_2)/\xi_\parallel]}{\sinh^2(L/\xi_\parallel)}\right]\right\}. \quad \text{(A10)}$$

The two-dimensional structure factor in a constant-z cross section is obtained from Eq. (A10) by letting $z_1=z_2$,

$$S_{2T}(q_\perp,z_1)=\frac{n_0k_BT}{B_3\xi_\parallel}\frac{1}{B_2+B_3\xi_\parallel F(L/\xi_\parallel)}$$
$$\times\left\{B_3\xi_\parallel+B_2\coth(L/\xi_\parallel)-\frac{B_2B_3\xi_\parallel}{B_2+B_3\xi_\parallel\coth(L/\xi_\parallel)}\frac{\cosh[(2z_1-L)/\xi_\parallel]}{\sinh(L/\xi_\parallel)}\right\}. \quad \text{(A11)}$$

For $z_1=L$ and $z_1=0$ this is identical to the expression given in Eq. (1.9).

It is interesting to consider the correlation of density fluctuations on the two opposite surfaces of the sample, corresponding to the three-dimensional structure function of (A10) for $z_1=L$ and $z_2=0$. From Eq. (A10) we obtain

$$S_T(q_\perp,L,0)=S_{2T}(q_\perp,0)R(q_\perp,L)\ , \quad \text{(A12)}$$

where $S_{2T}(\mathbf{q}_\perp,0)=S_{2T}(q_\perp,L)$ is the two-dimensional structure factor of one of the two surfaces, and

$$R(q_\perp,L)=\frac{B_3\xi_\parallel}{B_2\sinh(L/\xi_\parallel)+B_3\xi_\parallel\cosh(L/\xi_\parallel)} \quad \text{(A13)}$$

measures the correlations between flux-line patterns at the two opposite ends of the sample. If the size of the sample is small compared to the correlation length, $L\ll\xi_\parallel$, flux lines are straight throughout the sample and $R(q_\perp,L)\approx1$. The patterns on the two surfaces are perfectly correlated in this limit. Conversely, if $L\gg\xi_\parallel$, the patterns on the two surfaces are uncorrelated and $R(q_\perp,L)\approx0$. A measure of the deviation of $R(q_\perp,L)$ from 1 would give us information about the degree of flux-line wandering in the superconductor.

[1] M. C. Marchetti and D. R. Nelson, Physica C **174**, 40 (1991).

[2] For a review see D. R. Nelson, in *Phenomenology and Applications of High-Temperature Superconductors,* edited by K. S. Bedell *et al.* (Addison-Wesley, Reading, MA, 1992).

[3] D. S. Fisher, M. P. A. Fisher, and D. Huse, Phys. Rev. B **43**, 130 (1991).

[4] D. S. Fisher, in *Phenomenology and Applications of High-Temperature Superconductors* (Ref. 2).

[5] P. L. Gammel, D. J. Bishop, G. J. Dolan, J. R. Kwo, C. A. Murray, L. F. Schneemeyer, and J. V. Waszczak, Phys. Rev. Lett. **59**, 2592 (1987).

[6] G. J. Dolan, G. V. Chandrasekar, T. R. Dinger, C. Field, and F. Holtzberg, Phys. Rev. Lett. **62**, 827 (1989).

[7] C. A. Murray, P. L. Gammel, D. J. Bishop, D. B. Mitzi, and A. Kapitulnik, Phys. Rev. Lett. **64**, 2312 (1990).

[8] D. G.Grier, C. A. Murray, C. A. Bolle, P. L. Gammel, D. J. Bishop, D. B. Mitzi, and A. Kapitulnik, Phys. Rev. Lett. **66**, 2270 (1991).

[9] P. L. Gammel, in *Phenomenology and Applications of High-Temperature Superconductors* (Ref. 2) and references therein.

[10] M. C. Marchetti and D. R. Nelson, Phys. Rev. B **41**, 1910 (1990).

[11] E. M. Chudnovsky, Phys. Rev. B **43**, 7831 (1991).

[12] J. Pearl, J. Appl. Phys. **37**, 4139 (1966).

[13] D. A. Huse, Phys. Rev. B **46**, 8621 (1992).

[14] D. R. Nelson and S. Seung, Phys. Rev. B **39**, 9153 (1989).

[15] D. R. Nelson and P. LeDoussal, Phys. Rev. B **42**, 10 113 (1990).

[16] As pointed out in Ref. 4, the single-line tilt coefficient contains a term that survives even in the limit of very large anisotropy and was missed in much previous literature. Using the results of Ref. 4, one obtains $\tilde{c}_{44}(0)=(n_0\phi_0^2/16\pi^2\lambda_{ab}^2)\{\ln(\gamma\kappa)/\gamma^2-[1/(2\gamma^2)]+(\frac{1}{2})\}$. Here λ_{ab} and $\lambda_c=\gamma\lambda_{ab}$ are the penetration lengths in the ab plane and along the $\hat{\mathbf{c}}$ axis, respectively, with γ the anisotropy parameter. Also, $\kappa=\lambda_{ab}/\xi_{ab}$, with ξ_{ab} the coherence length in the ab plane.

[17] The reader may question the consistency of approximating the elastic constants by their values at $q_z=0$, while retaining their dependence on $q_\perp$. It turns out that the main effect of the nonlocality on the properties of interest here is that of reducing the value of the bulk modulus at $q_\perp\sim1/a_0$, as compared to its value at $q_\perp=0$. This effect is retained in the approximation used here.

[18] D. R. Nelson, Physica A **177**, 220 (1991).

[19] M. C. Marchetti, Physica C **200**, 155 (1992).

[20] The highest fields probed in the decoration are of the order of 100 G. For applied fields along the $\hat{\mathbf{c}}$ axis diamagnetization corrections are large in the thin samples used in the experiments. As a result $B\simeq H$, even for $H<H_{c1}$.

[21] We note that since we are using a hydrodynamic theory we are always discussing wave vectors $q_\perp<G_0$, where $G_0=2\pi(2/\sqrt{3}n_0)^{1/2}$ is the shortest reciprocal lattice vector of the triangular Abrikosov lattice, corresponding to the location of the first peak of the two-dimensional structure function.

[22] C. A. Murray (private communication).

[23] E. H. Brandt, J. Low Temp. Phys. **42**, 557 (1981).

[24] O. Buisson, G. Carneiro, and M. Doria, Physica C **185-189**, 1465 (1991).

[25] R. Lipowsky, Phys. Rev. Lett. **49**, 1575 (1982).